Archimedean, Logarithmic and Euler spirals – intriguing and ubiquitous patterns in nature

DANILO R. DIEDRICHS

1. *Introduction and background*

Spirals are among the most intriguing of geometrical patterns, frequently encountered in the world around us at all scales, from the cosmic spiral arms of galaxies to the microscopic structure of the DNA molecule. For centuries, humans have studied these patterns, classifying them, giving them different names, and describing them mathematically. The most common definition of a two-dimensional spiral is a curve on the plane traced by a point that winds around a certain fixed point (called the spiral's *pole*), while monotonically approaching or receding from it, depending on the direction of motion. This definition can be expanded by relaxing the monotonicity condition, or by extending it to three dimensions. This paper focuses on the three major families of two-dimensional spirals encountered in the world around us: Archimedean spirals (Section 2), logarithmic spirals (Section 3), and Euler spirals (Section 4). Although spirals are well documented in the literature, the sheer number of different types and names can be confusing to the novice. This paper aims at providing an organised and clear exposition of the three main families, tracing their historical background, highlighting their similarities and differences, and displaying the wide range of applications for each type.

Spirals are often described by an equation written in polar coordinates r (distance from the origin) and θ (polar angle), with the spiral's pole at the origin. Because, according to our definition, a spiral must approach or recede from its pole monotonically, the function $r = r(\theta)$ in polar coordinates must be continuous and monotonic. Cartesian parametric equations $x(t)$ and $y(t)$ can be derived from the polar equation $r(\theta)$ by setting

$$\begin{aligned} x(t) &= r(t)\cos t \\ y(t) &= r(t)\sin t \end{aligned},$$

where the parameter t plays the role of the polar angle θ.

The Cartesian equations, in turn, can be used to define the *arc length coordinate* at any point on the curve

$$s(t) = \int_0^s \sqrt{dx^2 + dy^2} = \int_0^s \sqrt{x'(t)^2 + y'(t)^2}\, dt,$$

which is the distance measured along the curve from the point where $t = 0$. The arc length coordinate s is a more meaningful parameter than t (the polar angle), and also has the advantage of being an *intrinsic* parameter, as it does not depend on the coordinate system. Therefore spirals (and parametric curves in general) are often reparametrised according to their arc length coordinate s.

https://doi.org/10.1017/mag.2019.7 Published online by Cambridge University Press

Another intrinsic quantity which can be defined at every point of a parametric curve is the *curvature* κ, which measures how fast the curve is turning at that point. If ψ is the angle between the tangent to the curve and the horizontal axis, then the curvature is the rate of change of ψ with respect to the arc length $\left(\kappa = \frac{d\psi}{ds}\right)$. Equivalently, the curvature is the inverse of the *radius of curvature* $\rho = \left|\frac{ds}{d\psi}\right|$ of the given curve at a point, which is the radius of the tangent circle with the same curvature (called the *osculating circle* by Leibniz). In Cartesian coordinates, the curvature is given by:

$$\kappa = \frac{x'(t)\,y''(t) - y'(t)\,x''(t)}{(x'(t)^2 + y'(t)^2)^{3/2}}. \tag{1}$$

Because the arc length and curvature are intrinsic quantities, the equation $\kappa = \kappa(s)$ (called the Cesàro equation of a curve) can recreate the curve independently of a coordinate system. In the case of a spiral, similarly to the function $r = r(\theta)$, the function $\kappa = \kappa(s)$ is also continuous and monotonic. The Cesàro equation is the simplest way to describe the Euler spiral (see Section 4).

2. *Archimedean spirals*

Archimedean spirals are named after Archimedes, who described a spiral of this type in his treatise *On spirals* in the third century BC. Although the spiral itself was first studied by Archimedes' friend and fellow mathematician Conon of Samos, Archimedes employed it to solve two classical geometry problems: squaring the circle and trisecting an angle. These two ancient problems were later (19th century) proved to be impossible to solve just with a straightedge and compasses, the only permissible tools in classical geometry.

The general equation of an Archimedean spiral in polar coordinates is a linear equation of the form

$$r = a + b\theta^n, \tag{2}$$

where a, b and n are constants. Several subcategories of Archimedean spirals have their own name, depending on the number n. The most common ones are explained below: the arithmetic spiral ($n = 1$), the hyperbolic spiral ($n = -1$), the Fermat spiral ($n = \frac{1}{2}$), and the lituus ($n = -\frac{1}{2}$).

Arithmetic spiral

The general equation of an arithmetic spiral is

$$r = a + b\theta. \tag{3}$$

It describes the trajectory of a point moving at constant speed along a ray spinning around the origin at constant angular velocity. Archimedes used a spiral of this type with $a = 0$ in *On spirals*, so these spirals are also called *Spirals of Archimedes* (see Figure 1 for an arithmetic spiral with $a = 0$ and $b = 1$). The classic arithmetic spiral usually only refers to the branch for

https://doi.org/10.1017/mag.2019.7 Published online by Cambridge University Press

positive values of θ ($0 < \theta < \infty$). However if the polar angle is allowed to span from $-\infty$ to ∞, the full spiral with both branches is called a *neoid* or *swan-like curve*.

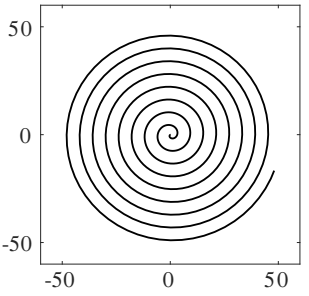


FIGURE 1:
Arithmetic spiral $r = \theta$

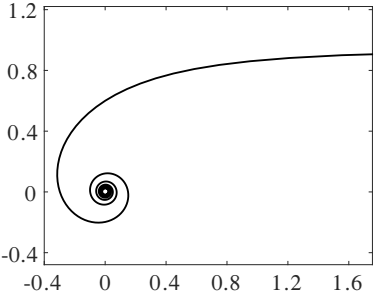


FIGURE 2:
Hyperbolic spiral $r = 1/\theta$

A ray originating with a polar angle θ_k intersects an arithmetic spiral in at a distance from the origin $r_k = a + b\theta_k$. The same ray will intersect the spiral on the next turn at a distance $r_{k+1} = a + b(\theta_k + 2\pi) = r_k + 2\pi b$. Thus the ray will intersect the spiral in a sequence of points with constant separation distance $2\pi b$. The distance of these points from the origin is given by the recurrence relation $r_{k+1} = r_k + 2\pi b$ which defines an *arithmetic sequence*, hence the name of this spiral.

Because arithmetic spirals are connected to the trajectory of a point in motion, they appear naturally in dynamic spirals involving points moving outward on a rotating disc spinning with constant angular velocity, such as the pattern made by a spiral platter in microbiology experiments, or by a Catherine wheel firework. Furthermore, because arithmetic spirals have constant separation distance between successive coils, they appear naturally in any system that involves wrapping a string or thin membrane around an axis, such as a roll of paper or tape around a cylinder, the grooves of a gramophone record, or the balance springs used in mechanical clocks and watches.

Hyperbolic spiral

The general equation of a hyperbolic spiral is

$$r = a + b\theta^{-1}. \tag{4}$$

As with the arithmetic spiral, the hyperbolic spiral is usually restricted to the branch obtained with only positive values of θ. Figure 2 shows a hyperbolic spiral with $a = 0$ and $b = 1$.

The hyperbolic spiral begins at infinity and approaches the origin along the horizontal asymptote $y = b$, as can be seen by finding the limit of the parametric y-coordinate as $\theta \to 0^+$:

$$\lim_{\theta \to 0^+} y(\theta) = \lim_{\theta \to 0^+} r(\theta) \sin\theta = \lim_{\theta \to 0^+} \left(a + \frac{b}{\theta}\right) \sin\theta = b.$$

https://doi.org/10.1017/mag.2019.7 Published online by Cambridge University Press

As $\theta \to \infty$, the spiral asymptotically approaches a circle of radius a around the origin (or the origin itself, if $a = 0$).

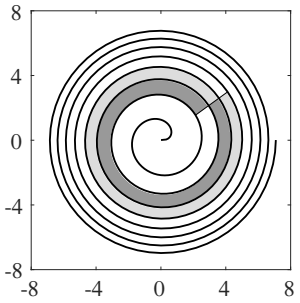


FIGURE 3:
Fermat spiral $r = \sqrt{\theta}$
The light and dark grey annuli have the same area.

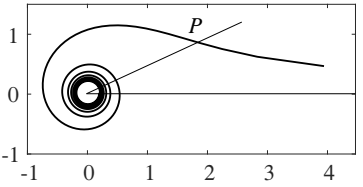


FIGURE 4:
Lituus $r = \theta^{-1/2}$
The point of inflection P is at the point where the polar angle is $\theta = \frac{1}{2} \approx 28.65°$.

Fermat spiral

The Fermat spiral is named after the French mathematician Pierre de Fermat, as he was the first to study it in 1636. The general equation is

$$r = b\sqrt{\theta}. \tag{5}$$

Rewriting the equation as $r^2 = b^2\theta$ results in adding a second branch, symmetric to the first one about the origin. Figure 3 shows a Fermat spiral with $b = 1$.

A Fermat spiral has the property of enclosing equal areas with every turn. Let A_0 be the area enclosed by the spiral at polar angle θ_0.

$$A_0 = \tfrac{1}{2}\int_{\theta_0 - 2\pi}^{\theta_0} r(\theta)^2\, d\theta = \tfrac{1}{2}b^2 \int_{\theta_0 - 2\pi}^{\theta_0} \theta\, d\theta = b^2\pi\left(\theta_0 - \pi\right).$$

At the next turn, the area will be

$$A_1 = \tfrac{1}{2}\int_{\theta_0}^{\theta_0 + 2\pi} r(\theta)^2\, d\theta = \tfrac{1}{2}b^2 \int_{\theta_0}^{\theta_0 + 2\pi} \theta\, d\theta = b^2\pi\left(\theta_0 + \pi\right).$$

Therefore the area of the annulus between two successive turns is constant:

$$A_1 - A_0 = 2b^2\pi^2.$$

For this reason, the Fermat spiral appears in disc phyllotaxis when studying the arrangement of seeds in disc-like flowers such as a daisy or sunflower. As these plants grow, they produce seeds at the centre of the flower that push the other seeds outward. In addition, the location of each newly produced seed is at a constant polar angle relative to the previous seed. So if every seed is assumed to have the same area then they naturally become arranged at a constant spacing along a Fermat spiral.

The relative angle α between two successive seeds (called the *divergence angle*), causes secondary spiral patterns (called *parastichies*) to

https://doi.org/10.1017/mag.2019.7 Published online by Cambridge University Press

emerge. By far the most common divergence angle observed in plants is about 137.5°, called the *golden angle* because it is related to the golden section of the circumference of a circle $\alpha = \frac{360°}{\varphi} \approx 222.5°$ (or equivalently 137.5° in the other direction), where φ is the golden ratio $\frac{1}{2}(1 + \sqrt{5})$. It can be shown that this angle produces the most efficient packing of seeds in the smallest area, so plants may have evolved to naturally adopt this angle for efficiency in their seed placement [1, 2, 3, 4, 5]. This same divergence angle appears in phyllotaxis, i.e. the placement of leaves on a plant stem. One hypothesis is that, assuming that the sun and rain come from above, perpendicular to the plane of the leaves, an irrational divergence angle avoids any periodicity which would cause higher leaves to block sun and rain from the lower leaves. And since the golden ratio is the most irrational number, we arrive at the optimal divergence angle of 137.5° [6]. Recent research has also suggested that this divergence angle minimises the energy cost of twisting the stem [7].

Lituus

The name of this spiral comes from the fact that this spiral looks like a Roman lituus, a crooked staff similar to a bishop's crosier. The general equation of a lituus is

$$r = b\theta^{-1/2}. \tag{6}$$

As with the Fermat spiral, rewriting the equation as $r^2\theta = b^2$ results in adding a second branch, symmetric to the first one about the origin. Figure 4 shows a lituus with $b = 1$.

The lituus begins at infinity and approaches the origin along the horizontal asymptote $y = 0$, as can be seen by finding the limit of the parametric y-coordinate as $\theta \to 0^+$:

$$\lim_{\theta \to 0^+} y(\theta) = \lim_{\theta \to 0^+} r(\theta) \sin\theta = \lim_{\theta \to 0^+} \frac{\sin\theta}{\sqrt{\theta}} = 0.$$

The lituus has an inflection point, which is the point where the curvature $\kappa(\theta)$ is zero:

$$\kappa(\theta) = \frac{\left|r(\theta)^2 + 2r'(\theta)^2 - r(\theta)\,r''(\theta)\right|}{\left(r(\theta)^2 + 2r'(\theta)^2\right)^{3/2}} = 4\theta^2 - 1 = 0.$$

Solving this equation yields the location of the inflection point $(r_0, \theta_0) = (b\sqrt{2}, \frac{1}{2})$.

Finally the lituus has the property that when a point P moves along it, the area of the circular sector between the horizontal asymptote and a circle going through P remains constant and equal to $\frac{1}{2}b^2$.

https://doi.org/10.1017/mag.2019.7 Published online by Cambridge University Press

3. *Logarithmic spirals*

The general equation of a logarithmic spiral is

$$r = ae^{b\theta}, \tag{7}$$

where a and b are constants. Its name comes from the fact that taking the logarithm on both sides of this converts it to a linear equation in θ:

$$\ln r = \ln a + b\theta.$$

Figure 5 shows a logarithmic spiral with $a = 1$ and $b = 0.1$. Logarithmic spirals have many properties, as described below.

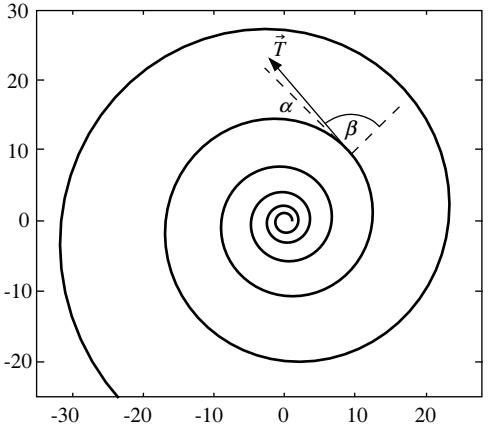


FIGURE 5: Logarithmic spiral $r = e^{0.1\theta}$ with a constant pitch $\alpha \approx 5.71°$

Self-similarity

One of the fundamental properties of a logarithmic spiral is self-similarity, meaning that its shape remains the same when scaled by a constant (up to a rotation by a constant angle). Indeed, scaling a logarithmic spiral by a constant k gives the equation

$$kr = kae^{b\theta} = ae^{\ln k}e^{b\theta} = ae^{b\left(\theta + \frac{\ln k}{b}\right)},$$

which is the same as the original spiral, but rotated clockwise by the angle $\frac{\ln k}{b}$. So although the size of the spiral changes, its shape does not. The shape is uniquely defined by the parameter b, which describes how tightly it winds around the origin. (At the limit when $b = 0$, the spiral degenerates to a circle). The multiplicative parameter a merely defines the angle by which the spiral is rotated around the origin.

The logarithmic spiral was first described by Descartes, and later by Jacob Bernoulli, who was so fascinated by it that he called it *Spira mirabilis*, which is Latin for 'the miraculous spiral' or 'wondrous spiral'. He even requested that a logarithmic spiral be engraved on his headstone with the phrase *Eadem mutata resurgo*, which means 'Although changed, I will arise

https://doi.org/10.1017/mag.2019.7 Published online by Cambridge University Press

the same', in reference to the resurrection of the dead when we will arise with a similar form, but with a new, changed body. Unfortunately however, because of an engraving error, Bernoulli's headstone was engraved with an Archimedean spiral instead.

Geometric progression

A ray originating with a polar angle θ_k intersects a logarithmic spiral a distance from the origin $r_k = ae^{b\theta_k}$. The same ray will intersect the spiral on the next turn at a distance $r_{k+1} = ae^{b(\theta_k + 2\pi)} = r_k e^{2\pi b}$. Thus the ray will intersect the spiral in a sequence of points whose distance from the origin is given by the recurrence relation $r_{k+1} = r_k e^{2\pi b}$ which defines a *geometric sequence* (in contrast with the arithmetic sequence obtained with the arithmetic spiral).

Constant pitch

The parametric Cartesian equations of a logarithmic spiral are

$$\begin{cases} x(t) = ae^{bt}\cos t \\ y(t) = ae^{bt}\sin t \end{cases},$$

and can be used to define the position vector $\vec{r}(t) = \begin{bmatrix} x(t) \\ y(t) \end{bmatrix}$ and the tangent vector $\vec{r}'(t) = \begin{bmatrix} x'(t) \\ y'(t) \end{bmatrix}$ at any point on the curve. A remarkable property of the logarithmic spiral is that the angle β between these two vectors is constant, as can be seen by taking their dot product:

$$\vec{r}(t)\cdot\vec{r}'(t) = \left\|\vec{r}(t)\right\| \left\|\vec{r}'(t)\right\| \cos\beta,$$

yielding

$$\beta = \operatorname{Arccos}\frac{\vec{r}(t)\cdot\vec{r}'(t)}{\left\|\vec{r}(t)\right\| \left\|\vec{r}'(t)\right\|} = \operatorname{Arccos}\frac{b}{\sqrt{1+b^2}}.$$

Because this angle depends only on b, it remains constant along the spiral. Another common and intuitive way of defining a logarithmic spiral is by its *pitch angle* α, which is the complement of β $(\alpha = 90° - \beta)$. Because the pitch angle is constant, a logarithmic spiral is often called an *equiangular spiral*.

Golden spiral

A golden spiral is a special case of a logarithmic spiral that grows by the golden ratio $\varphi = \frac{1}{2}(1+\sqrt{5})$ for every quarter turn. To find the parameter b in the equation of a golden spiral $r(\theta) = ae^{b\theta}$, we set

$$r\left(\theta + \tfrac{1}{2}\pi\right) = \varphi r(\theta),$$

https://doi.org/10.1017/mag.2019.7 Published online by Cambridge University Press

which yields $b = \frac{2 \ln \varphi}{\pi}$ (approximately 0.306), corresponding to a pitch angle of approximately 17.0°.

There are several spirals that approximate the golden spiral. One of them is obtained by partitioning a golden rectangle (i.e. a rectangle whose ratio of its sides is the golden ratio) into a square and a similar golden rectangle. This smaller rectangle can be partitioned in the same way, continuing indefinitely, until the original rectangle is completely partitioned into smaller and smaller squares. Inscribing a quarter circle into each square results in a discrete spiral that approximates the golden spiral (see Figure 6).

Another approximation is the Fibonacci spiral, which is constructed differently, starting with two adjacent squares, then recursively adding another, larger, square onto the longest side of the resulting rectangle. The Fibonacci spiral is formed by connecting quarter circles inscribed in each square. The sides of the squares constructed in this way naturally form the Fibonacci sequence (1,1,2,3,5,8,13,21, etc.), and since the ratio between consecutive Fibonacci numbers approaches the golden ratio as they approach infinity, this spiral approaches the golden spiral as it grows (see Figure 7).

Because these approximations of the golden spiral consist of connected quarter circles, their curvature function $\kappa = \kappa(s)$ is not continuous (as the curvature jumps at each juncture).

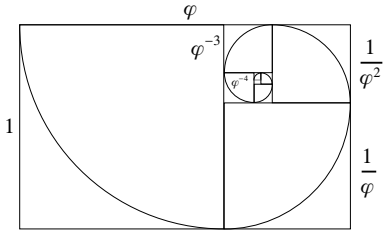


FIGURE 6:
Spiral built by partitioning a golden rectangle into squares

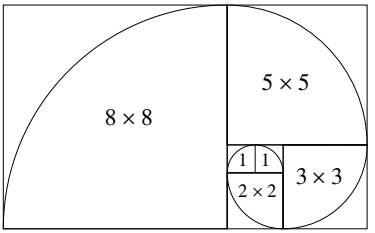


FIGURE 7:
Fibonacci spiral

Logarithmic spirals in nature

Logarithmic spirals are the most common type of spiral observed in nature at all scales, from the cosmically large to the microscopic. The arms of spiral galaxies form logarithmic spirals; our own Milky Way is an example with a constant pitch of approximately 12 degrees. This is a consequence of a disc rotating as a fluid about its centre, with the angular velocity increasing closer to the centre [8]. Similarly, the arms of tropical cyclones also form logarithmic spirals. Interestingly, logarithmic spirals are also found in the shape of the shoreline at certain beach fronts (called *logarithmic spiral beaches*); approaching wave fronts are refracted and curve as a result of diffraction at the headland, causing the shoreline to bend

https://doi.org/10.1017/mag.2019.7 Published online by Cambridge University Press

into the shape of a logarithmic spiral [9, 10, 11]. At the microscopic level, the nerves in the cornea in certain animals (e.g. rats and mice) exhibit the shape of a logarithmic spirals [12, 13].

Recent research has revealed that falcons and other birds of prey use logarithmic spirals when attacking their prey. Because its eyes are on either side of its head, the falcon does not have the clearest vision of its prey when it is head-on, but rather at an angle of about 40 degrees with the angle of its head. Rather than cocking its head (which would induce significant aerodynamic drag), the falcon instead maintains the 40 degree angle between its line of sight and flight path during approach, thereby creating an equiangular spiral [14]. Similarly, logarithmic spirals are observed in the flight path of the luna moth and many similar nocturnal insects who navigate by maintaining a constant angle between their flight path and the brightest light source in the night sky, which is usually the moon (infinitely far away), allowing the moth to fly in a straight line. But if a nearby lamp outshines the moon, the moth is drawn to it instead, and approaches it as an equiangular spiral [15].

The self-similarity property of logarithmic spirals causes it to appear in a large number of organisms that replicate their shape in increasing sizes as they grow, a growth process called *gnomonic growth*. The chambered nautilus, a marine mollusc with a snail-like shell divided into several chambers (as many as 30), provides a typical example. As it grows, the nautilus builds its shell longer and wider to accommodate its growing body, eventually producing a wall to seal off the old chamber. The new chamber is larger than the old one, but proportionally similar to it, thereby producing a logarithmic spiral [16, 17]. This same growth pattern can be seen in the growth of animal horns, nails, and tusks, as well as in plants such as Romanesco broccoli and cauliflower [18].

4. *Euler spiral*

Euler spirals have the characteristic property that their curvature varies linearly with the arc length. They were developed independently at least three times, in the context of different applications. In 1694, Jacob Bernoulli posed a problem about the behaviour of elastic springs, which Euler solved in 1744 using this spiral that now bears his name. In 1818, Augustin Fresnel, while studying the patterns resulting from light emanating from a nearby source diffracting through a slit (a phenomenon called *Fresnel diffraction*), developed two integrals that are equivalent to the parametric equations that generate the Euler spiral. In the late 19th century, railway engineers were faced with the necessity of designing a railway transition curve with gradual curvature variation along the arc, thereby once again deriving the same equation that had been developed earlier by Bernoulli, Euler, and Fresnel.

This spiral is also called the *Cornu spiral*, after the French physicist Alfred Marie Cornu, who developed the spiral as a graphical aid to evaluate the Fresnel integrals. Another common name for this curve is the *clothoid*,

https://doi.org/10.1017/mag.2019.7 Published online by Cambridge University Press

the name given to it by the Italian mathematician Ernesto Cesàro in reference to Clotho, one of the three Fates of Greek mythology who spins the thread of life around her distaff.

Cesàro equation

The Cesàro equation of a curve defines its curvature κ as a function of its arc length coordinate s (whose origin is a point on the curve which must be defined). It is an intrinsic equation, defining a relationship between the curve's intrinsic properties without referring to an arbitrarily-defined coordinate system. The curvature of the Euler spiral increases linearly with the arc length, so its Cesàro equation is

$$\kappa(s) = as, \tag{8}$$

where a is a constant. Figure 8 shows an Euler spiral with $a = 1$ (for $0 \leqslant s < \infty$).

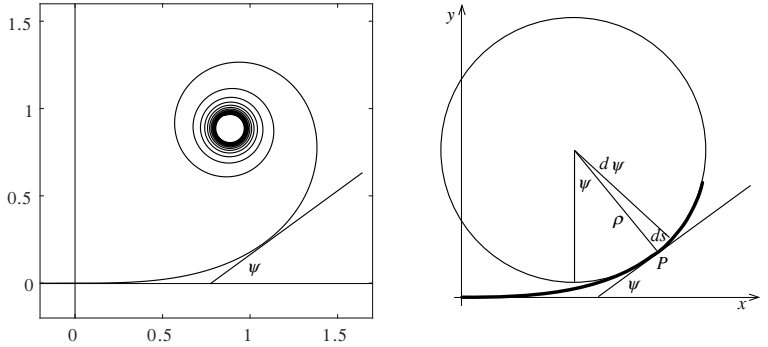


FIGURE 8: Euler spiral $\kappa = s$ (for $0 \leqslant s < \infty$) and diagram showing the construction of the parametric equations

Parametric equations and the Fresnel integrals

Figure 8 shows a sketch that resembles one that Euler himself used in his construction of the spiral [19]. Calling ψ the angle that the tangent to the spiral at a point P makes with the horizontal axis, and ρ the radius of the osculating circle at P, we see that $ds = \rho\, d\psi$. And since the radius of the osculating circle is the inverse of the curvature κ, we can use equation (8) to obtain the simple differential equation $d\psi = as\, ds$, whose solution is

$$\psi = \tfrac{1}{2}as^2, \tag{9}$$

assuming that $\psi = 0$ when $s = 0$. To find the parametric equations for the Cartesian coordinates x and y, we note that $\dfrac{dx}{ds} = \cos\psi$ and $\dfrac{dy}{ds} = \sin\psi$,

https://doi.org/10.1017/mag.2019.7 Published online by Cambridge University Press

which, together with equation (9), give us the following integral equations, called the *Fresnel integrals*:

$$\begin{aligned} x(s) &= \int_0^s \cos \tfrac{1}{2}at^2\, dt \\ y(s) &= \int_0^s \sin \tfrac{1}{2}at^2\, dt \end{aligned}, \tag{10}$$

assuming that $x = y = 0$ when $s = 0$.

Although the length of the Euler spiral is infinite, it reaches an asymptotic limit point (x_ℓ, y_ℓ) as $s \to \infty$. The coordinates of this point can be found by evaluating the limits of the Fresnel integrals:

$$\begin{aligned} x_\ell &= \int_0^\infty \cos \tfrac{1}{2}at^2\, dt = \sqrt{\frac{\pi}{4a}} \\ y_\ell &= \int_0^\infty \sin \tfrac{1}{2}at^2\, dt = \sqrt{\frac{\pi}{4a}} \end{aligned}.$$

Euler's method for solving these integrals is described in [19]. They can also be evaluated using Fourier series [20] or by contour integration in the complex plane.

Applications

The fact that the Euler spiral has been discovered multiple times by people working in different fields is a testament to the wide applicability of this spiral. Both Bernoulli and Euler discovered it while studying the curvature of a thin band of an elastic material, such as spring metal. Later, Fresnel rediscovered the spiral in his work involving the patterns of light diffracting through a slit.

Perhaps the most widely use of the Euler spiral nowadays is in civil engineering, more specifically in railway and road construction, as a transition curve between a straight line ($\kappa = 0$) and a circular arc ($\kappa =$ constant). A mass m moving along a curve at constant speed v experiences a centripetal force at every point on the curve equal to $F_c(s) = mv^2\kappa(s)$, where $\kappa(s)$ is the instantaneous curvature at the arc length coordinate s. So if a circular arc were connected directly to a straight line segment, the curvature would suddenly change from zero to a non-zero constant (the circle's curvature) at the juncture, and a vehicle travelling on the curve would be subjected to a large jerk, causing discomfort to passengers and dangerous levels of stress on the vehicle's mechanical parts. This could be a cause of road accidents and train derailments. Therefore an Euler spiral is inserted between the straight line segment and the circular arc to provide a gradual increase in centripetal force.

Following the same principle, Euler spirals are used in the design of upside-down moving roller coasters, where the teardrop-shaped loop uses two, spliced Euler spirals (called a clothoid loop) on either side of a circular arc, providing a gradual increase and decrease of g-forces experienced by

https://doi.org/10.1017/mag.2019.7 Published online by Cambridge University Press

passengers. Similarly, the trajectory of experienced racetrack drivers, as they optimise their racing line during the entry portion of a corner, has been shown empirically to approach an Euler spiral [21].

5. *Conclusion*

This discussion on spirals can be extended by relaxing the requirement that the polar function $r = r(\theta)$ or curvature function $\kappa = \kappa(s)$ be continuous and monotonic, leading for example to curves obtained by splicing different curves (as in the Fibonacci spiral), constructing spirals built on ellipses, or even curves that intersect themselves. Furthermore, spirals can be extended into the third dimension in a variety of ways, winding on the surface of a cylinder, cone, or sphere, for example, leading to helices or vortices which can be described by equations in cylindrical or spherical coordinates, parametric Cartesian coordinates, or by a relationship between its intrinsic quantities: arc length, curvature, and torsion.

References

1. G. J. Mitchison, Phyllotaxis and the Fibonacci Series: an explanation is offered for the characteristic spiral leaf arrangement found in many plants, *Science, New Series*, **196** (4287) (1977) pp. 270-275.
2. Michael Naylor, Golden, $\sqrt{2}$ and π flowers: a spiral story, *Mathematics Magazine*, **75** (3) (2002) pp.163-172.
3. Ivars Peterson, Golden blossoms, Pi flowers, *Science News* (2002) https://www.sciencenews.org/node/20073
4. Ivars Peterson, Fermat's natural spirals, *Science News* (2005) https://www.sciencenews.org/article/fermats-natural-spirals
5. Helmut Vogel, A better way to construct the sunflower head, *Mathematical Biosciences*, **44** (1979) pp. 179-189.
6. K. K. Tung, *Topics in mathematical modeling*, Princeton University Press (2007).
7. Takuya Okabe., Biophysical optimality of the golden angle in phyllotaxis, *Scientific Reports*, **5**:15358 (2015).
8. Benjamin L. Davis *et al*, Measurement of galactic logarithmic spiral arm pitch angle using two-dimensional fast Fourier transform decomposition. *The Astrophysical Journal Supplement Series*, **199**(33) (2012) pp. 1-20.
9. J. M. Bremner, Properties of logarithmic spiral beaches with particular reference to Algoa Bay, in *Sandy beaches as ecosystems: based on the Proceedings of the First International Symposium on Sandy Beaches, held in Port Elizabeth, South Africa*, Springer Netherlands (1983) pp. 97-113.
10. D. M. Chapman, Zetaform or logarithmic spiral beach, *Australian Geographer*, **14**(1) (1978) pp. 44-45.

https://doi.org/10.1017/mag.2019.7 Published online by Cambridge University Press

11. Paul H. LeBlond, An explanation of the logarithmic spiral plan shape of headland-bay beaches. *Journal of Sedimentary Petrology*, **49**(4) (1979) pp. 1093-1100.
12. T. Mohammad Nejad, S. Iannaccone, W. Rutherford, P. M. Iannaccone, and C. D. Foster, Mechanics and spiral formation in the rat cornea, *Biomechanics and Modeling in Mechanobiology*, **14**(1) (January 2015) pp. 22-38.
13. Jerry Rhee, Talisa Mohammad Nejad, Olivier Comets, Seam Flannery, Eine Begum Gulsoy, Philip Iannaccone and Craig Foster, Promoting convergence: The Phi spiral in abduction of mouse corneal behaviours, *Complexity*, **20**(3) (January 2015) pp. 22-38.
14. Vance Tucker., Gliding flight: drag and torque of a hawk and a falcon with straight and turned heads, and a lower value for the parasite drag coefficient, *The Journal of Experimental Biology*, **203**(Pt 24):3733-44 (December 2000).
15. Khristo N. Boyarzhiev, Spirals and conchospirals in the flight of insects. *The College Mathematics Journal*, **30**(1) (1999) pp. 23-31.
16. Gary Meisner, Is the Nautilus shell spiral as a golden spiral? (2014) https://www.goldennumber.net/nautilus-spiral-golden-ratio
17. Gary Meisner, Spirals and the Golden Ratio (2012) https://www.goldennumber.net/spirals/
18. Mario Livio, *The golden ratio: the story of Phi, the world's most astonishing number*, Broadway Books (2002).
19. Nick Lord, Euler, the clothoid and $\int_0^\infty \frac{\sin x}{x} dx$, *Math. Gaz.*, **100** (July 2016) pp. 266-273.
20. G. J. O. Jameson, Evaluating Fresnel-type integrals, *Math. Gaz.*, **99** (November 2015) pp. 491-498.
21. Adam Brouillard, *Perfect corner: a driver's step-by-step guide to finding their own optimal line through the physics of racing*, Paradigm Shift Motorsports Books (2016).

10.1017/mag.2019.7

DANILO R. DIEDRICHS

Department of Mathematics and Computer Science, Wheaton College, 501 College Avenue, Wheaton, IL 60187 USA

e-mail: *danilo.diedrichs@wheaton.edu*

https://doi.org/10.1017/mag.2019.7 Published online by Cambridge University Press